

Unbinned angular analysis of $B^0 \rightarrow K^{*0} \mu^+ \mu^-$ decays

Martin Andersson¹, Ulrik Egede², Tom Hadavizadeh², **Riley Henderson**², Zahra Moghaddam³,
Partick Owen¹, Kostas Petridis³, Eluned Smith⁴, Rongrong Song²

¹University of Zurich

²Monash University

³University of Bristol

⁴Massachusetts Institute of Technology



University of
Zurich^{UZH}



MONASH
University



University of
BRISTOL



Massachusetts
Institute of
Technology

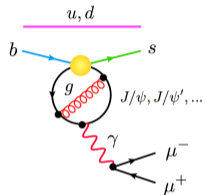
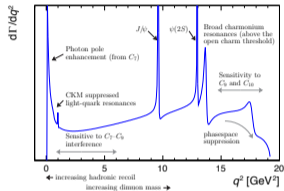
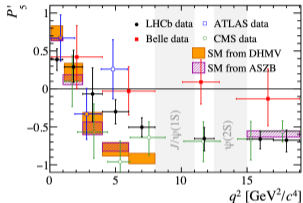
- 1 Introduction and recap
- 2 Overview of the analysis
 - Amplitude model
 - Dataset and selection requirements
 - Detector acceptance and resolution
- 3 Fitting strategy
- 4 Checks and validations
- 5 Systematic uncertainties
- 6 Summary

- 1 Introduction and recap
- 2 Overview of the analysis
 - Amplitude model
 - Dataset and selection requirements
 - Detector acceptance and resolution
- 3 Fitting strategy
- 4 Checks and validations
- 5 Systematic uncertainties
- 6 Summary

- Current discrepancies in binned $B^0 \rightarrow K^{*0} \mu^+ \mu^-$ angular observables could be due either to New Physics (NP) in the vector coupling C_9 , or to unaccounted contributions from interference with $c\bar{c}$ states.

$$\frac{d^4\Gamma}{dq^2 d^3\Omega}$$

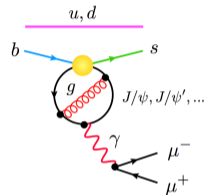
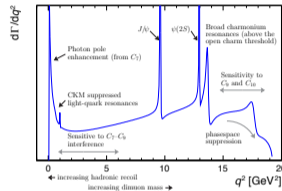
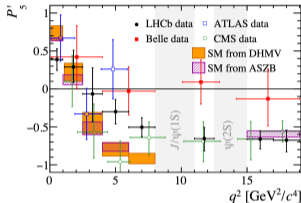
$$\equiv \frac{9}{32\pi} \sum_i J_i(q^2) f_i(\cos\theta_\ell, \cos\theta_K, \varphi)$$



- Current discrepancies in binned $B^0 \rightarrow K^{*0} \mu^+ \mu^-$ angular observables could be due either to New Physics (NP) in the vector coupling C_9 , or to unaccounted contributions from interference with $c\bar{c}$ states.

$$\frac{d^4\Gamma}{dq^2 d^3\Omega}$$

$$= \frac{9}{32\pi} \sum_i J_i(q^2) f_i(\cos\theta_\ell, \cos\theta_K, \varphi)$$



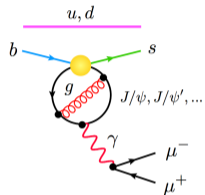
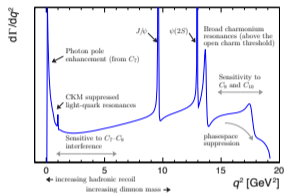
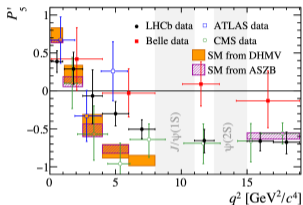
How can we disentangle NP from SM hadronic physics?

- In the face of *anomalous results*, one usually tries to deduce the values of the Wilson coefficients from the angular observables to find ΔC_i^{NP} — the shift due to NP contributions.

- Current discrepancies in binned $B^0 \rightarrow K^{*0} \mu^+ \mu^-$ angular observables could be due either to New Physics (NP) in the vector coupling C_9 , or to unaccounted contributions from interference with $c\bar{c}$ states.

$$\frac{d^4\Gamma}{dq^2 d^3\Omega}$$

$$= \frac{9}{32\pi} \sum_i J_i(q^2) f_i(\cos\theta_\ell, \cos\theta_K, \varphi)$$

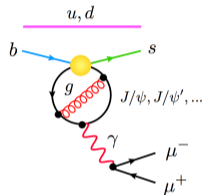
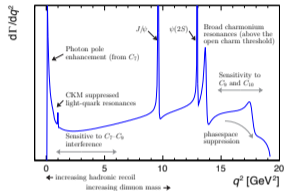
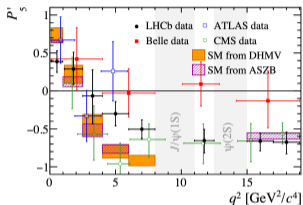


How can we disentangle NP from SM hadronic physics?

- In the face of *anomalous results*, one usually tries to deduce the values of the Wilson coefficients from the angular observables to find ΔC_i^{NP} — the shift due to NP contributions.
- This requires theoretical input for hadronic form factors which can cause effective shifts in the Wilson coefficients — and the theoretical uncertainties for these are non-negligible.

- Current discrepancies in binned $B^0 \rightarrow K^{*0} \mu^+ \mu^-$ angular observables could be due either to New Physics (NP) in the vector coupling C_9 , or to unaccounted contributions from interference with $c\bar{c}$ states.

$$\frac{d^4\Gamma}{dq^2 d^3\Omega} = \frac{9}{32\pi} \sum_i J_i(q^2) f_i(\cos\theta_\ell, \cos\theta_K, \varphi)$$



How can we disentangle NP from SM hadronic physics?

- In the face of *anomalous results*, one usually tries to deduce the values of the Wilson coefficients from the angular observables to find ΔC_i^{NP} — the shift due to NP contributions.
- This requires theoretical input for hadronic form factors which can cause effective shifts in the Wilson coefficients — and the theoretical uncertainties for these are non-negligible.
- We aim, instead, to empirically measure the size and level of interference of these hadronic contributions, $\Delta C_i^{\text{SM}}(q^2)$, to disentangle them from ΔC_i^{NP} .

- 1 Introduction and recap
- 2 Overview of the analysis
 - Amplitude model
 - Dataset and selection requirements
 - Detector acceptance and resolution
- 3 Fitting strategy
- 4 Checks and validations
- 5 Systematic uncertainties
- 6 Summary

- We parameterise the signal based on the $B^0 \rightarrow K^{*0} \mu^+ \mu^-$ transversity amplitudes:

$$A_0^{L,R}(q^2) = -8N \frac{m_B m_{K^*}}{\sqrt{q^2}} \left(([C_9^{(\text{eff}),0}(q^2) - C_9'] \mp [C_{10} - C_{10}']) A_{12}(q^2) + \frac{m_b}{m_B + m_{K^*}} C_7^{(\text{eff}),0} T_{23}(q^2) \right),$$

$$A_{\parallel}^{L,R}(q^2) = -N\sqrt{2}(m_B^2 - m_{K^*}^2) \left(([C_9^{(\text{eff}),\parallel}(q^2) - C_9'] \mp [C_{10} - C_{10}']) \frac{A_1(q^2)}{m_B - m_{K^*}} + \frac{2m_b}{q^2} C_7^{(\text{eff}),\parallel} T_2(q^2) \right),$$

$$A_{\perp}^{L,R}(q^2) = N\sqrt{2}\lambda \left(([C_9^{(\text{eff}),\perp}(q^2) + C_9'] \mp [C_{10} + C_{10}']) \frac{V(q^2)}{m_B + m_{K^*}} + \frac{2m_b}{q^2} C_7^{(\text{eff}),\perp} T_1(q^2) \right),$$

$$A_t(q^2) = \frac{N}{\sqrt{q^2}} \sqrt{\lambda} \left(2[C_{10} - C_{10}'] A_0(q^2) \right),$$

$$A_{00}^{L,R}(q^2) = -N \frac{\lambda_{K^*0}}{\sqrt{q^2}} \sqrt{q^2} \left((C_9^{(\text{eff}),00}(q^2) \mp C_{10}) F_1(q^2) + \frac{2m_b}{m_B + m_{K^*}} C_7^{(\text{eff}),00} F_T(q^2) \right).$$

- We parameterise the signal based on the $B^0 \rightarrow K^{*0} \mu^+ \mu^-$ transversity amplitudes:

$$A_0^{L,R}(q^2) = -8N \frac{m_B m_{K^*}}{\sqrt{q^2}} \left(([C_9^{(\text{eff}),0}(q^2) - C_9'] \mp [C_{10} - C_{10}']) A_{12}(q^2) + \frac{m_b}{m_B + m_{K^*}} C_7^{(\text{eff}),0} T_{23}(q^2) \right),$$

$$A_{\parallel}^{L,R}(q^2) = -N\sqrt{2}(m_B^2 - m_{K^*}^2) \left(([C_9^{(\text{eff}),\parallel}(q^2) - C_9'] \mp [C_{10} - C_{10}']) \frac{A_1(q^2)}{m_B - m_{K^*}} + \frac{2m_b}{q^2} C_7^{(\text{eff}),\parallel} T_2(q^2) \right),$$

$$A_{\perp}^{L,R}(q^2) = N\sqrt{2}\lambda \left(([C_9^{(\text{eff}),\perp}(q^2) + C_9'] \mp [C_{10} + C_{10}']) \frac{V(q^2)}{m_B + m_{K^*}} + \frac{2m_b}{q^2} C_7^{(\text{eff}),\perp} T_1(q^2) \right),$$

$$A_t(q^2) = \frac{N}{\sqrt{q^2}} \sqrt{\lambda} \left(2[C_{10} - C_{10}'] A_0(q^2) \right),$$

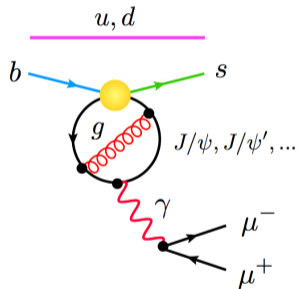
- Local P-wave form factors.
- Local S-wave form factors.
- Effective Wilson coefficients — *i.e.* including non-local form factors.

$$A_{00}^{L,R}(q^2) = -N \frac{\lambda_{K^*0}}{\sqrt{q^2}} \sqrt{q^2} \left((C_9^{(\text{eff}),00}(q^2) \mp C_{10}) F_1(q^2) + \frac{2m_b}{m_B + m_{K^*}} C_7^{(\text{eff}),00} F_T(q^2) \right).$$

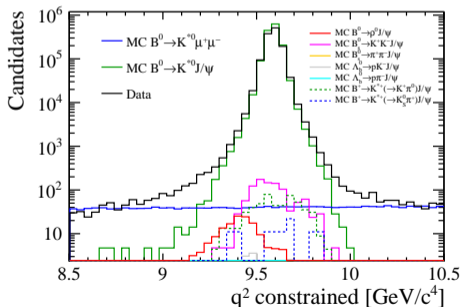
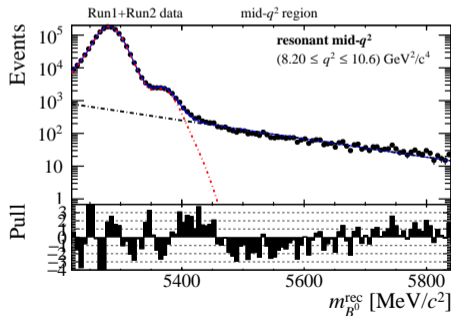
- We consider a number of non-local contributions to C_9 :

$$C_9^{\text{eff},\lambda}(q^2) = C_9 + Y_{q\bar{q}}(q^2)$$

- The non-local term, $Y_{q\bar{q}}$, covers all of the relevant intermediate states in $q\bar{q} \rightarrow \mu^+\mu^-$
- This includes:
 - 1 particle states: ϕ (1020), J/ψ , $\psi(2S)$, ...
 - 2 particle states: $D\bar{D}$, D^*D , D^*D^* , $\tau^+\tau^-$.

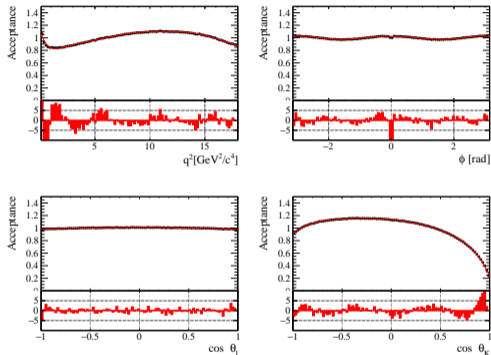


- We use the combined Run 1 + Run 2 LHCb dataset¹ corresponding to 8.4 fb^{-1} .
- Our selection requirements are mostly aligned with the ongoing *binned angular analysis* to facilitate comparisons — except we do not exclude the resonance dominated regions.
- We remove both exclusive peaking backgrounds and combinatorial background using BDTs and some explicit vetos.



¹Excluding 2015 which is a small contribution with unsuitable conditions.

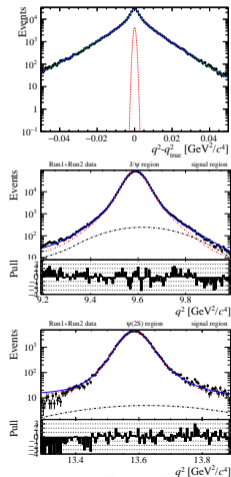
The detector acceptance is well modelled in simulation.



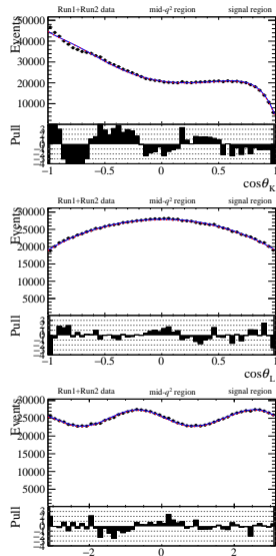
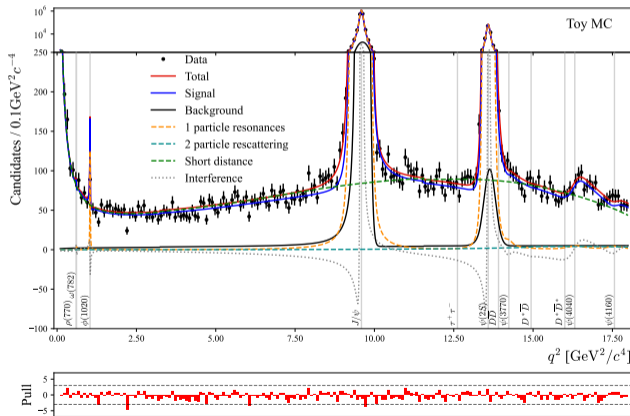
Legendre polynomial models

| Variable | Max Order | Symmetric |
|--------------------|-----------|-----------|
| q^2 | 9 | |
| $\cos \theta_K$ | 7 | |
| $\cos \theta_\ell$ | 4 | |
| ϕ | 6 | ✓ |

The detector q^2 resolution is modelled using a combination of simulated and real data.



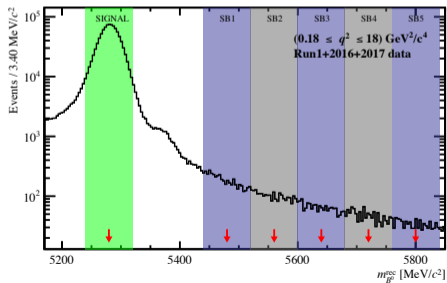
- (left) fit to a toy dataset showing the full description of the q^2 spectrum.
- (right) fits to data showing the angular dimensions.



- 1 Introduction and recap
- 2 Overview of the analysis
 - Amplitude model
 - Dataset and selection requirements
 - Detector acceptance and resolution
- 3 Fitting strategy**
- 4 Checks and validations
- 5 Systematic uncertainties
- 6 Summary

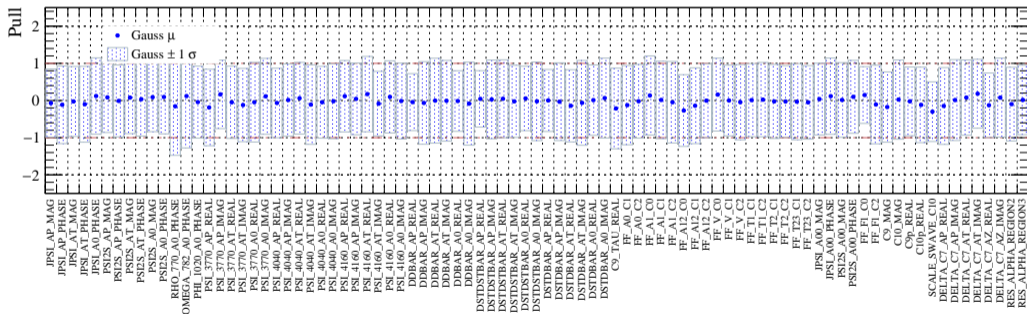
Three steps of the fit:

- 1 Fit to full $m_{B^0}^{rec} \equiv m_{K\pi\mu\mu}$ range — [5220 GeV, 5840 GeV] — to extract the signal fractions and combinatorial background slopes in each region.
- 2 Fit to the upper $m_{B^0}^{rec}$ side-band — [5440 GeV, 5840 GeV] — to determine the background shape parameters in $\cos\theta_\ell$, $\cos\theta_K$, φ , and q^2 .
- 3 Fit to the signal region — [5239.58 GeV, 5319.58 GeV] — with full signal plus background model.



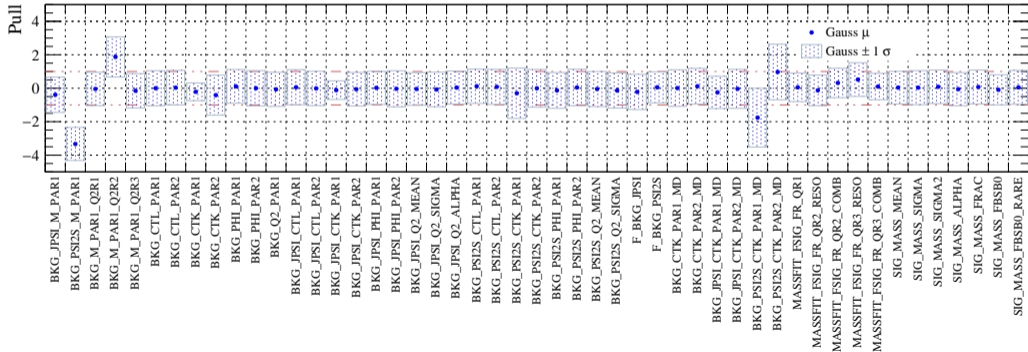
- 1 Introduction and recap
- 2 Overview of the analysis
 - Amplitude model
 - Dataset and selection requirements
 - Detector acceptance and resolution
- 3 Fitting strategy
- 4 Checks and validations
- 5 Systematic uncertainties
- 6 Summary

- Altogether we float a total of 135 parameters ← 87 signal + 37 bkg + 5 signal fractions + 6 signal mass parameters.
- Pull plots in toy studies look well behaved and fit stability is good:



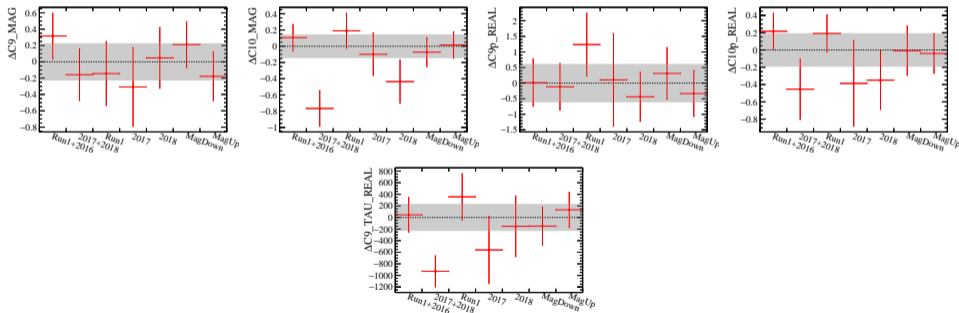
Gaussian mean μ (blue points) and width σ (blue boxes) of the pull distributions for each signal parameter.

- Altogether we float a total of 135 parameters ← 87 signal + 37 bkg + 5 signal fractions + 6 signal mass parameters.
- Pull plots in toy studies look well behaved and fit stability is good:



Gaussian mean μ (blue points) and width σ (blue boxes) of the pull distributions for each signal parameter.

- We have cross checked the fit stability by fitting various subsets of the full dataset:
 - Split into Run1+2016 and 2017+2018
 - Split into Run1, 2016, 2017, 2018
 - Split by magnet polarity.



- The results are mostly very consistent — we are investigating the $\mathcal{O}(3\sigma)$ differences in C_{10} and C_9^T in the 2017 + 2018 fit.

- We have measured the values of the P-wave angular observables obtained in bins around the J/ψ and $\psi(2S)$ resonance pole masses.
- We compare these values to the ongoing binned angular analysis and to previous LHCb measurements at the J/ψ mass:

| Observable | J/ψ | | |
|------------|----------------------|----------------------|--------------------|
| | Unbinned | Binned | LHCb 2011 |
| F_L | 0.5580 ± 0.0006 | 0.5586 ± 0.0006 | 0.572 ± 0.008 |
| S_3 | -0.0069 ± 0.0008 | -0.002 ± 0.0008 | -0.013 ± 0.010 |
| S_4 | -0.2450 ± 0.0005 | -0.2447 ± 0.0009 | -0.250 ± 0.006 |
| S_8 | -0.0558 ± 0.0009 | -0.0511 ± 0.0009 | -0.048 ± 0.007 |
| S_9 | -0.0922 ± 0.0009 | -0.0861 ± 0.0008 | -0.084 ± 0.006 |

| Observable | $\psi(2S)$ | |
|------------|----------------------|----------------------|
| | Unbinned | Binned |
| F_L | 0.518 ± 0.002 | 0.5213 ± 0.0025 |
| S_3 | -0.0159 ± 0.0043 | -0.0100 ± 0.0033 |
| S_4 | -0.200 ± 0.003 | -0.1847 ± 0.0036 |
| S_8 | -0.0987 ± 0.0049 | -0.0802 ± 0.0038 |
| S_9 | -0.213 ± 0.003 | -0.1842 ± 0.0032 |

- For the $\psi(2S)$, there are noticeable tensions in S_3 and S_9 between the binned and unbinned analyses; however, both are compatible with the previous measurement and the uncertainties here are statistical only.

- 1 Introduction and recap
- 2 Overview of the analysis
 - Amplitude model
 - Dataset and selection requirements
 - Detector acceptance and resolution
- 3 Fitting strategy
- 4 Checks and validations
- 5 Systematic uncertainties
- 6 Summary

The key sources of systematics uncertainty we have studied are:

- **normalisation to measured $B^0 \rightarrow J/\psi K^{*0}$ branching fraction** — **large** effect on C_9 and C_{10} (50–100% of stat. unc.).
- **residual peaking backgrounds** — **large** effect on J/ψ resolution tail parameters (80–90% of stat. unc.).
- **constraining the open-charm contributions** — **large** effect on $C_9^{(\tau)}$ J/ψ phase (30–40% of stat. unc.).
- **exotic charmonium-like resonances** — moderate bias corrections applied (20–30% of stat. unc. for C_9 and C_{10} , up to 100% for resonance phases) — uncertainty of correction is WIP.
- **decay angle resolution** — **small** effect on resonance phases (10–15% of stat. unc.).
- **variation in q^2 resolution** — **small** effect on C_7 (<10% of stat. unc.).
- **MC corrections on acceptance** — **small** effect on J/ψ magnitudes (5–10% of stat. unc.).
- Numerous other effects have been tested and found to be negligible...

- 1 Introduction and recap
- 2 Overview of the analysis
 - Amplitude model
 - Dataset and selection requirements
 - Detector acceptance and resolution
- 3 Fitting strategy
- 4 Checks and validations
- 5 Systematic uncertainties
- 6 Summary

The key points

- Direct unbinned fit to the 4D $B^0 \rightarrow K^{*0} \mu^+ \mu^-$ decay rate to extract Wilson coefficients.
- The goal is to give the fit all relevant degrees of freedom in the Standard Model and see how this affects the apparent New Physics shift in C_9 .

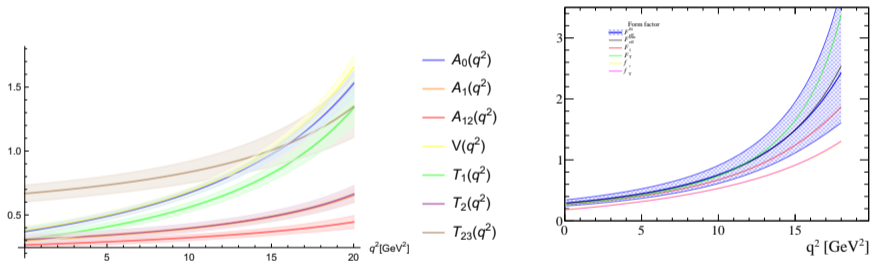
Where are we now?

- The analysis is currently under review by the rare decays working group in LHCb— no major concerns have been identified.
- We expect working group approval at the beginning of April — we will then begin collaboration wide review.
- The plan is to publish by mid-late 2023.

Thanks for listening!

Backup slides

- We parameterise the local form factors with a series expansion and allow the parameters to float in our fit to data.



- We apply theoretical constraints on the **P-wave form factors** calculated from Light Cone Sum Rules and Lattice QCD — Bharucha, Straub and Zwicky (2016)².

²New *improved* theory calculations of these form factors have been published recently in Gubernari, *et al.*. We will update our constraints accordingly but expect no significant changes.

- We do the fit in a small $K\pi$ mass window, $m_{K\pi}^2$, around the $K^{*0}(892)$ resonance.
- We therefore need to model the $m_{K\pi}^2$ lineshape which receives predominantly P-wave and S-wave contributions.
- Theoretical calculations of the local **S-wave form factors** have large/unknown uncertainties and we do not have sufficient sensitivity to the S-wave amplitudes to float them independently.
- We combine the two local S-wave form factors into a single effective form factor parameterised similarly to Doring, Meißner and Wang (2013).
- In order to avoid destroying sensitivity to the Wilson coefficients, we completely decouple the S-wave and P-wave amplitudes by introducing separate S-wave specific parameters for C_7 , C_9 , and C_{10} .
- The final form of the S-wave amplitude we fit for is thus:

$$\mathcal{A}_{00}^{L,R} = -N \frac{\lambda_{K_0^{*0}}}{\sqrt{q^2}} \left[F_{\text{eff}}(q^2) \left(C_9^{S(\text{eff})}(q^2) \mp C_{10}^S + \frac{2m_b}{m_{B^0} + m_{K^*}} C_7^S \right) \right]$$

- We model non-local contributions to \mathcal{C}_9 through a **once-subtracted hadronic dispersion relation**. The effective q^2 dependent Wilson coefficient is written as:

$$\mathcal{C}_9^{(\text{eff}),\lambda}(q^2) = \mathcal{C}_9 + Y^{q\bar{q},\lambda}(q^2)$$

where

$$Y^{q\bar{q},\lambda}(q^2) = Y^{q\bar{q}}(q_0^2) + \frac{q^2 - q_0^2}{\pi} \int_{q_{min}^2}^{\infty} ds \frac{\rho^{q\bar{q},\lambda}(s)}{(s - q_0^2)(s - q^2 - i\varepsilon)},$$

describes the $B^0 \rightarrow K^{*0}$ matrix element of the non-local charm-loop operator.

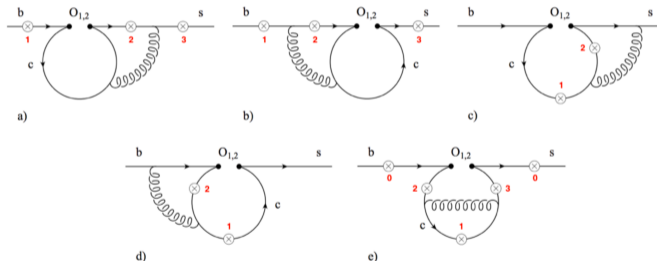
- The spectral density function $\rho^{q\bar{q},\lambda}(s)$ describes the intermediate hadronic states.

- We also include non-local contributions to \mathcal{C}_7 in the form of a constant (q^2 independent) but helicity dependent magnitude and phase shift.

$$\mathcal{C}_7^{(\text{eff}),\lambda} = C_7 + \zeta^\lambda e^{i\omega^\lambda}$$

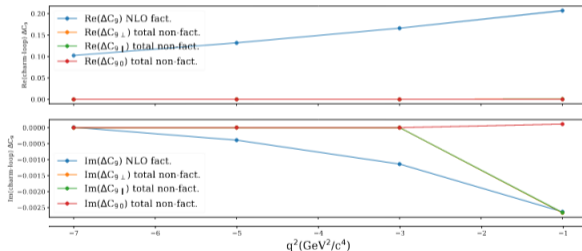
- We float two real degrees of freedom per helicity amplitude for each non-local contribution considered (with the exception of \mathcal{C}_9^τ which is assumed to be real and helicity independent).
- Additionally, the difference between the DD and D^*D contributions and the D^*D Gaussian constrained to zero for stability of the fit.
 - A cross-check has been performed for this constraint and it is

- The subtraction constant, $Y_{q\bar{q},\lambda}^{(0)} \equiv Y^{q\bar{q}}(q_0^2)$, is taken from theory calculations of the NLO *factorisable* contributions to the charm-loop by [Asatrian, Greub and Virto \(2020\)](#).

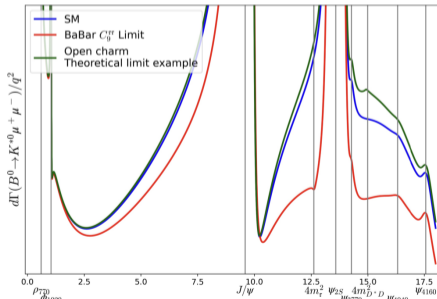


- The light-cone OPE based calculation is done for the (unphysical) value $q_0^2 = -4.6 \text{ GeV}^2$ where the OPE converges. The dispersion relation extrapolates this result to the physical q^2 region.

- We neglect the sub-dominant non-factorisable corrections which are found to be negligible in the q^2 region at which we perform the subtraction.

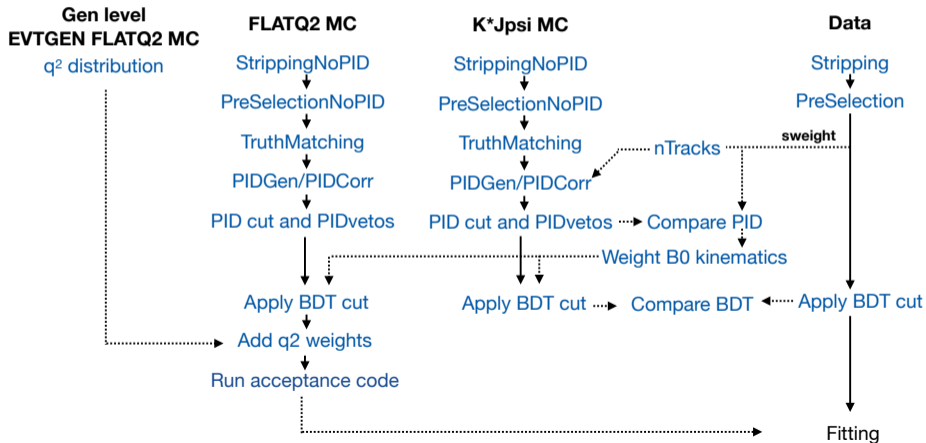


- Our sensitivity to C_9^T is currently at the level of around ± 285 based on toy studies — which should allow us to set a world's best limit on the size of this contribution.
 - The limit is currently $|C_9^T| \leq 910$ at 90% confidence level.
- We also have sensitivity to the open charm contributions but cannot freely float all components. We therefore constrain the difference of DD and D^*D^* components relative the D^*D to zero.
 - The D^*D has the largest lineshape and best sensitivity in our fit.
 - The constraint is fairly loose — width 1 — while our sensitivity is at the level of 0.4 for the D^*D , and 0.9 for the DD and D^*D^* .



- The **trigger** requirements are fairly standard, for example:
 - One or both muons must pass the L0 (di)muon hardware trigger, *i.e.* minimum p_T requirement.
 - High p_T tracks with large χ_{IP}^2 , *i.e.* *detached* from the PV.
 - Decay topology matching a multibody B decay with minimum 2 charged daughters.
- Likewise for the **pre-selection and stripping** requirements:
 - Displaced B decays with at least two muons and one hadron
 - Good quality track and vertex fits.
 - Loose PID requirements on kaons, pions, and muons.

- We use MC samples for $B^0 \rightarrow K^{*0} \mu^+ \mu^-$, $B^0 \rightarrow K^{*0} J/\psi$ and $B^0 \rightarrow K^{*0} \psi(2S)$ decays.
- These MC samples must be corrected for various differences between data and simulation.

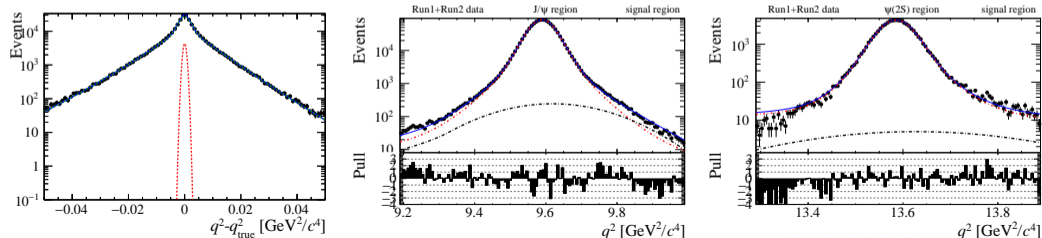


- The resolution in the decay angles $\cos \theta_\ell$, $\cos \theta_K$, and φ is **not** directly included in the signal model — we assign a systematic uncertainty for this
- The q^2 resolution is modelled as a Gaussian + two Crystal Ball functions:

$$\text{Res}(\Delta q^2) = f_{\text{CB}} \text{Gauss}(\Delta q^2, \sigma_{\text{Gauss}}) + \frac{1}{\mathcal{N}} (1 - f_{\text{CB}}) \left(\text{CB}(\Delta q^2, \sigma_{\text{CB}}, \alpha, n_{\text{upper}}) + \text{CB}(\Delta q^2, \sigma_{\text{CB}}, -\alpha, n_{\text{lower}}) \right)$$

where \mathcal{N} is a normalisation factor for the sum of opposite sided Crystal Ball functions.

- The resolution parameters are obtained in 3 separate q^2 regions through a staged combination of fits to both MC and data.



- The resolution and acceptance are applied to the theoretical decay rate as follows to obtain the final signal PDF:

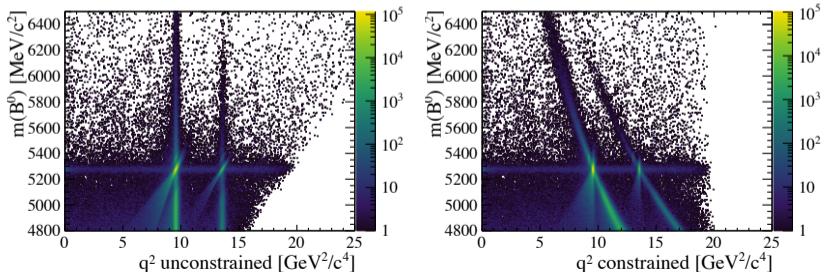
$$\mathcal{P}(q^2, \cos \theta_\ell, \cos \theta_K, \varphi) = \left(\frac{d^4 \Gamma}{dq^2 d^3 \Omega} \otimes \text{Res}(q^2 - q_{true}^2) \right) \times \epsilon(\cos \theta_\ell, \cos \theta_K, \varphi, q^2).$$

- The convolution with the resolution function is implemented via a Fast Fourier Transform (FFT).
- Note: the resolution is applied *before* the acceptance for reasons of computational complexity of the convolution. In the above, the convolution reduces to

$$\sum_{i=1}^{17} \left[J_i(q^2) \otimes \text{Res}(q^2 - q_{true}^2) \right] \quad \text{instead of} \quad \sum_{i=1}^{17} \sum_{n=0}^9 \left[J_i(q^2) P(q^2, n) \otimes \text{Res}(q^2 - q_{true}^2) \right]$$

We found the difference to be negligible given the relatively flat acceptance and relatively narrow resolution.

- We explicitly veto several peaking backgrounds — e.g. $B^+ \rightarrow K^+ \mu^+ \mu^-$, $\Lambda_b^0 \rightarrow p K^- \mu^+ \mu^-$, $B_s^0 \rightarrow \phi \mu^+ \mu^-$.
- The $B^+ \rightarrow K^+ \mu^+ \mu^-$ veto sculpts the $\cos \theta_K$, q^2 , and $m_{K\pi\mu\mu}$ distributions in the upper B^0 mass side-band. This is accounted for with an efficiency correction to the background PDF determined from phase space MC as discussed several times previously, e.g. [\[here\]](#) and [\[here\]](#).
- We consider three separate contributions to the combinatorial background: $B^0 \rightarrow K^{*0} \mu^+ \mu^-$, $B^0 \rightarrow J/\psi K^{*0}$, $B^0 \rightarrow \psi(2S) K^{*0}$.



- We use a B^0 mass constraint to improve the q^2 resolution — this also distorts the background and

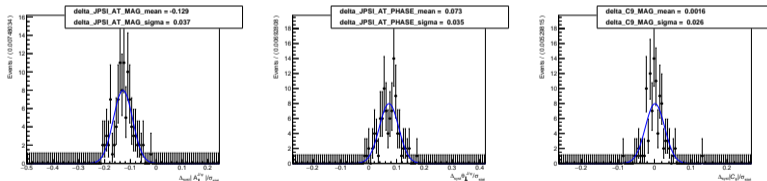
- We are blinding the Wilson coefficients C_9 , C'_9 , C_9^τ , C_{10} , C'_{10} .
- The blinding is implemented as:

$$C_i = C_i^{\text{SM}} + \text{sign} * \Delta C_i^{\text{NP}} + \text{offset}$$

where $\text{sign} \in \{-1, 1\}$ is a *random* sign flip of the shift due to NP and $\text{offset} \in [-0.5, 0.5]$ is a random blinding offset.

Angular resolution

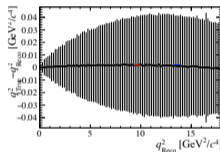
- We do not account for the angular resolution of the detector in our signal model — for simplicity and since the decay rate varies slowly in the angles.
- Toy studies revealed small biases in the J/ψ magnitude and phase entering the perpendicular amplitude $\sim 10\%$ of the corresponding statistical error.



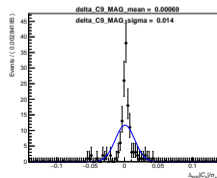
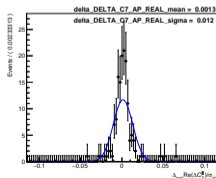
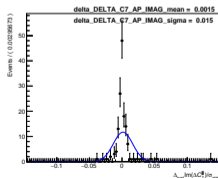
- Effects on all other parameters including Wilson coefficients were found to be very small.

Variation in q^2 resolution

- We fit simultaneously in three q^2 regions with a fixed resolution in each region; however, in reality the resolution varies significantly in some areas.

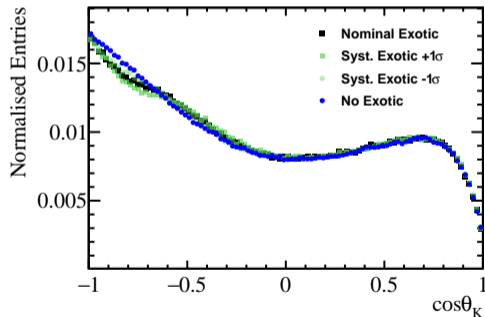


- Toy studies with the complete signal model indicated no significant systematic effects due to this.



Exotic charmonium-like states

- We ignore the presence of some exotic resonances in the $J/\psi\pi$ and $\psi(2S)\pi$ spectra which interfere with both the rare and resonant modes through $B \rightarrow Z(\rightarrow \psi\pi)K$.
- The most significant effect is seen in the $\cos\theta_K$ distribution around the J/ψ and $\psi(2S)$ resonances.



- We cannot simply include these contributions in our nominal model since they modify the angular distribution in a way that makes the FFT convolution in q^2 computationally infeasible.

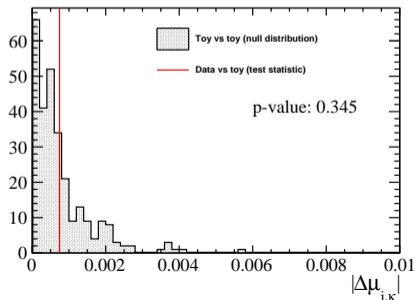
Correction for ignoring exotic charmonium-like states

- Toy studies with additional contributions from the $Z(4200)$ and the $Z(4430)$ resonances are used to **obtain a correction** for the absence of these states.
- In these toys we take the exotic amplitude parameters from measurements at Belle and BaBar — we account for the q^2 resolution by smearing the generated q^2 distribution.
- The most significant corrections are to the J/ψ and $\psi(2S)$ resonance phases along with smaller corrections to the Wilson coefficients:

| Parameter | Correction | Syst (frac of stat) |
|-------------------------------|------------|---------------------|
| $\theta_{J/\psi}^0$ | 5 mrad | WIP |
| $\theta_{\psi(2S)}^0$ | 60 mrad | WIP |
| $\theta_{J/\psi}^\perp$ | -8 mrad | WIP |
| $\theta_{\psi(2S)}^\perp$ | -90 mrad | WIP |
| $\theta_{J/\psi}^\parallel$ | -1 mrad | WIP |
| $\theta_{\psi(2S)}^\parallel$ | 18 mrad | WIP |
| C_9 | 0.07 | WIP |
| C_{10} | 0.04 | WIP |

- We will also obtain a systematic for the correction by varying the exotic amplitudes within their measured uncertainties.

- We have employed a BDT based goodness of fit test by generating toys from the (blinded) data best fit PDF.
- A set of BDTs are trained to distinguish the real data from the toy datasets, while another set of BDTs are trained to distinguish between different toys.
- The AUC is used as a performance metric for the BDTs.
- Averaging over many trained BDTs we find that the **toys generated from the data best fit PDF are generally indistinguishable from the real data!**



We will publish model dependent measurements of:

- **Wilson coefficients:** $C_9^{(\prime)}$, $C_{10}^{(\prime)}$
- **Local P-wave form factors:** A_0 , A_1 , A_{12} , V , T_1 , T_2 , T_{23}
- **Non-local amplitude parameters:**
 - $q\bar{q}$ resonance magnitudes and phases: $\rho(770)$, $\phi(1020)$, J/ψ , $\psi(2S)$, $\psi(3770)$, $\psi(4040)$, $\psi(4160)$ (one of each per helicity amplitude).
 - **Non-resonant magnitudes and phases:** ΔC_7 (one of each per helicity amplitude).
 - **Open-charm magnitudes and phases:** DD , D^*D , D^*D^* (one of each per helicity amplitude).
 - $\tau^+\tau^-$ -loop magnitude: C_9^τ
- **Resulting angular observables.**

What's left?

- We have recently made some changes to our nominal fit procedure — using a narrower B^0 mass signal region to remove events adversely affected by final state radiation.
- We need to reevaluate the systematic uncertainties following this change.

- Steps have been taken to allow inclusion of our results in the FLAVIO global fitting package:

